Clim. Past Discuss., 9, 2153–2181, 2013
www.clim-past-discuss.net/9/2153/2013/
doi:10.5194/cpd-9-2153-2013

Climate of the Past
Discussions
Open Access

Accumulation reconstruction and water isotope analysis for 1735–1997 of an ice core from the Ushkovsky volcano, Kamchatka, and their relationships to North Pacific climate records

T. Sato[1], T. Shiraiwa[1], R. Greve[1], H. Seddik[1], E. Edelmann[2], and T. Zwinger[2]

[1]Institute of Low Temperature Science, Hokkaido University, Kita-19, Nishi-8, Kita-ku, Sapporo 060–0819, Japan
[2]CSC – IT Center for Science, P.O. Box 405, 02101 Espoo, Finland

Received: 19 March 2013 – Accepted: 6 April 2013 – Published: 17 April 2013

Correspondence to: T. Sato (tsato@lowtem.hokudai.ac.jp)

Published by Copernicus Publications on behalf of the European Geosciences Union.

Abstract

To investigate past climate change in the Northwest Pacific region, an ice core was retrieved in June 1998 from the Gorshkov crater glacier at the top of the Ushkovsky volcano, in central Kamchatka. Hydrogen isotope (δD) analysis and past accumulation reconstructions were conducted to a depth of 140.7 m, dated to 1735. Two accumulation reconstruction methods were applied with the Salamatin and the Elmer/Ice ice flow models. Reconstructed accumulation rates and δD were significantly correlated with North Pacific surface temperature. This, and a significant correlation of δD with the North Pacific Gyre Oscillation (NPGO) index implies that NPGO data is contained in this record. Wavelet analysis shows that the ice core records have significant multi-decadal power spectra up to the late 19th century. The multi-decadal periods of reconstructed accumulation rates change at around 1850 in the same way as do Northeast Pacific ice core and tree ring records. The loss of multi-decadal scale power spectra of δD and the 6 ‰ increase in its average value occurred around 1880. Thus the core record confirms that the periodicity of precipitation for the entire North Pacific changed between the end of the Little Ice Age through the present due to changes in conditions in the North Pacific Ocean.

1 Introduction

Alpine ice core records have two important roles. One is to provide data for studying local climate characteristics. The other is to fill geographic gaps in the network of glacio-chemical and climatic records used to reveal how regions are affected by global climate change (Wagenbach, 1989; Cecil et al., 2004). There are several glacial regions around the North Pacific Ocean that might provide ice cores for paleoclimate reconstructions. The Ushkovsky/K2 ice core is one of two ice cores recovered from Kamchatka (Shiraiwa et al., 2001; Matoba et al., 2011). It is a paleoclimate record for this region that complements regional climate reconstructions from Alaskan ice cores

CPD
9, 2153–2181, 2013

(e.g. Holdsworth et al., 1989; Wake et al., 2002; Shiraiwa et al., 2003; Fisher et al., 2004; Yasunari et al., 2007).

Important characteristics of climate in the North Pacific region are decadal climate variabilities, the Pacific Decadal Variability or North Pacific Decadal Variability. One is the Pacific Decadal Oscillation (PDO), the first leading mode of North Pacific sea surface temperature variability (Mantua et al., 1997; Minobe, 1997). Another is the North Pacific Gyre Oscillation, the second mode of sea surface height anomalies (Di Lorenzo et al., 2008). These variabilities play important roles in modulating precipitation, temperature and other climatic elements around the North Pacific Ocean (e.g. Mantua and Hare, 2002; Di Lorenzo et al., 2008).

Because climate observations were not systematically recorded in this region until within the last 200 yr, investigation of long-term changes requires the use of paleoclimate proxies. North Pacific climate variability has therefore been reconstructed using tree rings from the Northeast Pacific region (e.g. Biondi et al., 2001; D'Arrigo et al., 2001). Summer mean maximum temperature reconstructed from Kunashir tree rings width indices (Jacoby et al., 2004) shows that the record is negatively correlated with the summer PDO index (Mantua et al., 1997) and has similar multi-decadal spectral properties. Climate variability has also been detected from glaciers in Alaska and Kamchatka that changed their mass balance at the climatic regime shifts in 1976/1977 (Hodge et al., 1998; Shiraiwa and Yamaguchi, 2002). Holdsworth et al. (1989) reconstructed accumulation rates at Mt. Logan and found a shift in the dominant period of the accumulation variations around 1850. Reconstructed snow accumulation increased notably after the mid 19th century, suggesting a relationship with the North Pacific climate (Moore et al., 2002).

To provide a further climate proxy for the western North Pacific we analysed water isotope ratios and reconstructed accumulation rates from the Ushkovsky/K2 ice core (Shiraiwa et al., 2001). Ushkovsky volcano (56.04° N, 160.28° E, 3903 m a.s.l.) is located in the central part of the Kamchatka Peninsula (Fig. 1). The summit of the volcano is covered by a glacier of 43 km^2. Two craters, Gorshkov and Herz, lie near the highest part and are both filled by glacier ice. The larger, Gorshkov, is ~ 750 m in diameter with maximum depth ~ 240 m determined by ice-penetrating radar (Matsuoka et al., 1999). In June 1998, at the K2 site near to this deepest point, a 211.7 m long ice core was drilled (Shiraiwa et al., 2001). It was the first ice core drilled in the western North Pacific region.

The firn temperature was measured continuously for a year at the BH1 site ~ 200 m south of K2. At 10 m depth the annual mean firn temperature is −15.8 °C. The monthly mean surface temperature is −5.8 °C at its maximum in August. Melting occurs only in the surface layer and the meltwater refreezes in the surface snow due to its low temperature. Melting does not, therefore, significantly disturb the annual stratigraphy conserved in the core (Shiraiwa et al., 2001). The average accumulation rate from 1969 to 1996 was determined as 0.57 m w.eq. a^{-1} by shallow ice core analysis (Shiraiwa et al., 1997).

The isotopes $\delta^{18}O$ and δD in the K2 core have already been analyzed from the surface to 110 m depth. The ice at this depth fell as snow in approximately 1823 based on dated layers of volcanic ash and counting of annual layers identified by changes in the water isotope ratio (Shiraiwa and Yamaguchi, 2002). In this study, we extended the record down to a depth of 140.7 m, dated to 1735. To determine accumulations, we applied two glacier flow models (Salamatin model, Salamatin et al., 2000, Elmer/Ice, Zwinger et al., 2007) to reconstruct annual layers down to the depth of the oldest dated volcanic ash layer (Murav'yev et al., 2007). Further, we carried out comparisons with local and large-scale climate data and investigated decadal and multi-decadal oscillations of the δD and accumulation records.

2 Methods

2.1 Isotope measurement and dating

The K2 ice core was sliced in order to take isotope measurements in the low temperature room (−20 °C) at the Institute of Low Temperature Science, Hokkaido University. To ensure that annual layers could be accurately identified, slices were taken at intervals small enough to provide at least eight samples for each annual layer. The intervals differed depending on the depth being 100 mm from the top down to 60.98 m, 50 mm from 60.98 to 110.3 m and 30 mm from 110.3 to 143.0 m. After slicing, each ice sample was melted in an individual sealed plastic bag. The resulting water was stored in 30–50 mL glass vials pending isotope measurements.

The water isotopes in slices taken from the first 110 m were measured with a Finnigan MAT Delta S mass spectrometer at the Graduate School of Environmental Science, Hokkaido University. Measurement errors were 0.1 ‰ for δ^{18}O and 1.02 ‰ for δD. The isotopes in slices from 110.0–140.7 m were measured at the Institute of Low Temperature Science. The δ^{18}O isotope was measured using a Finnigan Delta Plus mass spectrometer (measurement error 0.02–0.03 ‰), and δD using an Isoprime-PyrOH mass spectrometer (error 0.1 ‰). Two substandard water probes were used in each analysis, and results were corrected by the SMOW-SLAP scale (Hagemann et al., 1970).

The age of annual layers in the K2 core were dated by reference to four volcanic ash layers of known date (Murav'yev et al., 2007). The age of intervening layers was estimated by counting the annual layers as identified by locating the minimum in the seasonally varying amounts of δD. The four dated layers, of 328 in total, are for 1985 (at 12.04 m depth, Bezymianny eruption), 1956 (35.49 m, Bezymianny), 1829 (102.82 m, Klyuchevskoy) and 1737 (138.45 m, Bezymianny). The error of dating is ±2 yr at 102.82 m depth (Shiraiwa and Yamaguchi, 2002).

CPD
9, 2153–2181, 2013

2.2 Accumulation-rate reconstruction

The accumulation rate, the amount of snow fall per year, can be reconstructed by combining core data with models. The core data provide the age of the annual layers and their thickness. The thinning rate, how fast annual layers compact, can be estimated using ice flow models or measured vertical velocities in the glacier (Paterson and Waddington, 1984; Raymond et al., 1996; Schwerzmann et al., 2006). We applied two accumulation reconstruction methods; the Lagrangian back-trajectory method for the Salamatin model and the Eulerian method for the Elmer/Ice model.

2.2.1 Salamatin model

Salamatin et al. (2000) devised a firn/ice flow model for a crater glacier and applied it to Gorshkov. It is a thermo-mechanically coupled glacier flow-line model. Isotropic polycrystalline ice behaves as a linear viscous body at small stresses (Lipenkov et al., 1997; Salamatin et al., 1997). This linear rheology relating stress and strain rates (Salamatin and Duval, 1997) is included in the model. Using a normalized ice-equivalent vertical coordinate, analytical solutions for the velocities and consequently the strain rates can be obtained.

Trajectories of ice particles can be estimated if the velocity field is given. Therefore, it is possible to estimate the change of annual layer thicknesses in the glacier by using the back-trajectory method. The origin of each annual layer trajectory is set to its middle point. The end of the trajectory is set to the glacier surface. The backward trajectory of an annual layer is

$$\boldsymbol{r}(\boldsymbol{x}_{\mathrm{surf}}, t) = \boldsymbol{r}(\boldsymbol{x}_{z=c}, 0) - \int_0^t \boldsymbol{v}(\boldsymbol{x}, t)\,\mathrm{d}t\,. \qquad (1)$$

The surface position of an annual layer is obtained by its current position and the integral of the velocity along the trajectory. The negative sign indicates the backward

CPD
9, 2153–2181, 2013

direction along the trajectory. The vertical strain rate on each trajectory is estimated by

$$D_{zz}(\boldsymbol{x}) = \frac{\partial v_z(\boldsymbol{x})}{\partial z}. \quad (2)$$

The thinning rate is obtained by the integral of the vertical strain rate from its current to its end position,

$$\frac{1}{R(\boldsymbol{x})} = \exp\left(\int_0^{t_{\text{surf}}} D_{zz}\,\mathrm{d}t\right). \quad (3)$$

The accumulation rate for an annual layer at position $\boldsymbol{x}$ with thickness h (in metres of water equivalent) is

$$a_\mathrm{s} = \frac{h}{R(\boldsymbol{x})}. \quad (4)$$

2.2.2 Elmer/Ice

Elmer/Ice is a thermo-mechanically coupled, three-dimensional flow model (e.g. Gagliardini and Zwinger, 2008; Durand et al., 2009; Zwinger and Moore, 2009; Seddik et al., 2011, 2012) based on the open-source multi-physical simulation software Elmer (elmerice.elmerfem.org) that employs the finite element method. In the version used here (Zwinger et al., 2007), Elmer/Ice accounts for compressible firn (firn model by Gagliardini and Meyssonnier, 1997). It diagnostically solves the full Stokes equations for the Gorshkov crater glacier using the density profile from the K2 borehole and present-day surface temperature. We have improved the approach by Zwinger et al. (2007) in two major ways:

– In order to avoid the necessity of describing a boundary condition at the northern outflow of the crater glacier, we have added to the model domain a 500 m long downhill slab with a constant thickness of 50 m and a slope of 0.2 (estimated from the map shown in Fig. 2 of Shiraiwa and Yamaguchi, 2002).

– In parameterizing the geothermal heat flux (Zwinger et al., 2007, Eq. 27), we optimized the parameters q_{geo}^{min} (minimum geothermal heat flux at the deepest point of the crater glacier) and m (exponent of the bed elevation) for best agreement with the temperature measured and the age profiles at K2. Optimizing was carried out with APPSPACK ("Asynchronous Parallel Pattern Search") software and produced values of $q_{geo}^{min} = 17.578\,\mathrm{mW\,m^{-2}}$ and $m = 2.3359$.

Applying the model describes a velocity field in the north-south transect of the crater glacier through the K2 drillsite (Fig. 2).

In order to compute layer thinning in the Gorshkov glacier from the three-dimensional velocity field from the Elmer/Ice simulation, we defined the thinning function $R(\boldsymbol{x})$ as the ratio of the annual layer thickness at the position $\boldsymbol{x}$ in the glacier and at the surface, both counted in metres of ice equivalent (see also Eq. 3). It is equal to unity at the surface,

$$R|_s = 1\,, \tag{5}$$

and decreases with depth.

Whereas the computed velocity field accounts for compaction, this is neglected in the definition of the thinning function $R(\boldsymbol{x})$. Therefore, an auxiliary thinning function $\tilde{R}(\boldsymbol{x})$ is defined by

$$\tilde{R}(\boldsymbol{x}) = \frac{\rho_i}{\rho(d)} R(\boldsymbol{x})\,, \tag{6}$$

where $\rho_i = 910\,\mathrm{kg\,m^{-3}}$ is the density of pure ice and $\rho(d)$ the variable density of the firn at depth d. This function is governed by the equation

$$\frac{d\tilde{R}}{dt} = v_x \frac{\partial \tilde{R}}{\partial x} + v_y \frac{\partial \tilde{R}}{\partial y} + v_z \frac{\partial \tilde{R}}{\partial z} = \tilde{R} D_{zz}\,. \tag{7}$$

The vertical strain rate is given by $D_{zz} = \partial v_z / \partial z$. According to Eqs. (5) and (6) the surface boundary condition for Eq. (7) is

$$\tilde{R}|_s = \frac{\rho_i}{\rho_s}, \tag{8}$$

where ρ_s is the firn density at the glacier surface. We set $\rho_s = 0.45\,\rho_i$ (Zwinger et al., 2007).

We implemented the numerical solution of Eq. (7) for $\tilde{R}(\boldsymbol{x})$ in Elmer/Ice, and the original thinning function $R(\boldsymbol{x})$ results from Eq. (6). For a dated annual layer at position $\boldsymbol{x}$ with thickness h (in metres of ice equivalent), the accumulation rate a_s is given by Eq. (4).

3 Results

Annual layers were more than adequately sampled. There were 1461 samples covering the 170 yr 1828–1997, equivalent to 8.55 samples per annual layer. There were 1132 samples from the 91 yr 1736–1827, equivalent to 11.44 samples per layer.

Isotope measurements were hugely variable over the years (Fig. 3). The annual mean isotope ratio was estimated using the dating results (Fig. 4). The 20 yr running mean of δD is also shown. The average annual mean isotope ratio from 1736–1997 was −160.1 ‰. The 20 yr mean δD increased from the late 19th to the early 20th century. The value of δD is −156.1 ‰ from 1736 to 1880 and −162.1 ‰ from 1910 to 1997. The average value increased by 6.0 ‰ from 1880 to 1910. The multi-decadal δD fluctuation persisted from the early 18th century to the late 19th century and became weak in the 20th century.

Accumulation reconstruction using the two glacier flow models indicate that the ice at 140 m depth thins by a factor of 2 (water equivalent depth) in the Elmer/Ice model and by a factor of 1.5 in the Salamatin model (Fig. 5). The substantial difference between these two reconstruction methods is due to the different rheologies. The constitutive

CPD
9, 2153–2181, 2013

flow law used in Elmer/Ice is a power law which approaches the conventional Glen flow law with $n = 3$ in the limit of pure ice, whereas in the Salamatin model a linear rheology is assumed. The deeper ice is softer in the Elmer/Ice model than in the Salamatin model.

Accumulation rates have been stable (Salamatin) or show a slight increasing trend (Elmer/Ice) over the last 260 years (Fig. 6). The accumulation rates from 1736 to 1997 were 0.62 m w.eq. in the Elmer/Ice model, and 0.51 m w.eq. in the Salamatin model. There were clear multi-decadal fluctuations of both reconstructed accumulation rates (20 yr running mean). They were strong in ~ 1730–1850 and became weak after 1950.

4 Comparison with local climate data

We compared the annual mean δD with precipitation and air temperature records from the Kljuchi weather station (56.32° N, 160.83° E, approx. 40 m a.s.l., WMO Global Surface Network). Monthly precipitation (1961–1991) and monthly mean air temperature (1967–1989) were used to calculate the annual mean air temperature and annual total precipitation for the calendar year from January to December. The annual mean δD was not significantly correlated with the annual mean air temperature ($r = -0.22$) or the annual total precipitation ($r = -0.14$). The monthly-precipitation-weighted temperature (Steig et al., 1994) was derived to account for seasonal variation in precipitation. This was significantly correlated with the weighted annual mean temperature at Kljuchi station and δD ($r = 0.45$, $p < 0.05$) in 1967–1989. It suggests that δD reflects seasonal variation of precipitation rates and temperature though it is difficult to obtain a simple relationship between δD and temperature.

Reconstructed accumulation rates are not significantly correlated with annual precipitation rates (1961–1989) at Kljuchi ($r = -0.07$). The annual minimum δD cannot be dated to form a climate dataset; however, when the variability of the annual data was reduced by taking five-year running means of both the reconstructed accumulation rates and the precipitation rates at Kljuchi, a positive correlation of $r = 0.58$ emerged.

CPD
9, 2153–2181, 2013

The 20 yr mean reconstructed accumulation rates peak at 1810–1860, 1920 and 1970. The peaks of ∼ 1810–1860 and 1920 coincide with glacier advances on Kamchatka Peninsula in the mid 19th and early 20th century (Solomina et al., 1995). Increases around 1970 coincide with positive mass balances of glaciers in Kamchatka (Shiraiwa and Yamaguchi, 2002). Reconstructed annual accumulation from this ice core coincides to a degree with past winter accumulation rates reconstructed using a model of Koryto glacier. This glacier is located halfway up the east coast of Kamchatka (Yamaguchi et al., 2008). There are troughs around 1760–1770 followed by a steady increase to large values up to ∼1850. This again indicates that the reconstructed accumulation rate is related to the glacier advance and retreat history in the region.

5 Comparison with large-scale climate data

The δD signal and reconstructed accumulation rates were also compared with surface temperatures (ECMWF ERA40 reanalysis, 2 m monthly mean temperature fields). There is a significant positive correlation with mid-latitude North Pacific (20–40° N) surface temperatures, and a significant negative correlation with subpolar (40–60° N) North Pacific surface temperatures (Fig. 7a). The correlation map of reconstructed accumulation rates and ERA40 2 m air temperatures shows a significant negative correlation with the subpolar North Pacific (40–60° N, 180–150° W), and a significant positive correlation with the western coast of North America (40° N, 125° W and 60° N, 145° W) (Fig. 7b). This evidence indicates that the ice core records reflect North Pacific surface climate conditions.

The pattern of the correlation map of δD resembles the second leading mode of the North Pacific surface temperature (Bond et al., 2003), which is related to the North Pacific Gyre Oscillation (NPGO) (Di Lorenzo et al., 2010; Furtado et al., 2011). The correlation of annual mean δD with the annual mean NPGO index (Di Lorenzo et al., 2008) is $r = 0.27$ ($p < 0.10$) for 1950–1997 and $r = 0.70$ ($p < 0.01$) for 1979–1997. These

CPD
9, 2153–2181, 2013

results suggest that δD reflects the NPGO. The reconstructed accumulation rates also correlate to the NPGO index for 1950–1997 ($r = 0.29$, $p < 0.10$); however, for 1979–1997 the correlation is smaller than that for δD.

Water vapor transport analysis showed that almost 80 % of the precipitation over Eastern Siberia is contributed by the North Pacific during winter (December to February) and 50 % in summer (June to August) (Numaguti, 1999). The ocean is thus the main source of water vapor for the Kamchatka Peninsula, particularly in winter. The precipitation record at Kljuchi (1961–1997) shows that winter precipitation is higher than during other seasons, which suggests that there might be high winter precipitation ratios in the annual layers of the K2 ice core.

Since the main source of the ice in the core is precipitation from the North Pacific, the variation of water isotope ratio and reconstructed accumulation rates reflect the conditions of the region. The water isotope ratio of the precipitation depends on its sources and the condensation temperatures during transport (Dansgaard, 1964). Although variation in δD is caused by its dependency on the source conditions, this is not the only cause since it also depends on the precipitation weighted local temperature as suggested above. Detailed water isotope modelling analysis may improve understanding of its mechanism.

6 Wavelet analysis of δD and accumulation rates

Morlet wavelet analysis was applied to de-trended annual mean δD (Fig. 8a) and de-trended Elmer/Ice reconstructed accumulation rates (Fig. 8b) in order to examine decadal and multi-decadal oscillations and its variation. It was tested for significance at the 95 % confidence level against red noise (Torrence and Compo, 1998). The reconstructed accumulation rates derived by the Salamatin model and Elmer/Ice show similar patterns because the frequencies are not influenced much by the thinning rate corrections.

CPD
9, 2153–2181, 2013

The isotope δD has decadal (10–20 yr band) and multi-decadal significant coherences (40–60 yr band). Wavelet correlation of the multi-decadal domain decreases after ∼ 1840 and falls below the confidence interval at ∼1880. It matches the shift in average value of δD. Both mean values and the dominant periods of δD changed between the end of the Little Ice Age and the present. The coherence of the reconstructed accumulation rates also shows this change in significance. Multi-decadal significant coherence (40–60 yr band) found in ∼ 1740–1830 weakens thereafter. Then the 20–40 yr domain becomes significant in ∼ 1860–1940.

Some paleoclimatic proxies retrieved from the Western North Pacific also show the change of decadal time periods of precipitation related paleoclimatic records after the mid-19th century. Reconstructed accumulation rates derived from Mt. Logan ice core (Holdsworth et al., 1989) also show that the dominant time period changed in the mid 19th century. There was a 36 yr peak before 1860 but it became less significant after that period whereas there were 4, 11 and 21 yr peaks after 1880. Water isotope records of the Mt. Logan Eclipse ice core suggest the shift between mixed and zonal flow regimes of water vapor transport occurred around 1840 (Fisher et al., 2004). Tree ring records in Western North America (Gedalof and Smith, 2001; Gray et al., 2003) also show the shift of multi-decadal variabilities in mid-19th century. The match of the Ushkovsky/K2 ice core results with other paleoclimatic studies in this region demonstrates that the mid-19th century climate change affected both Northeast and Northwest Pacific surface precipitation conditions.

7 Conclusions

The comparison of δD from the Ushkovsky/K2 ice core with local meteorological data shows that data from the core reflect local temperature and seasonal precipitation. The average level of δD changed by 6.0 ‰ from 1737–1880 to 1910–1997. Although it would be caused by increases in average temperature from the end of the Little Ice

CPD
9, 2153–2181, 2013

Title Page
Abstract Introduction
Conclusions References
Tables Figures
◀| |▶
◀ ▶
Back Close
Full Screen / Esc
Printer-friendly Version
Interactive Discussion

Age to the present, it is difficult to ascertain a simple relationship between annual mean temperature and annual δD.

Lagrangian and Eulerian accumulation reconstruction using the Salamatin and Elmer/Ice models showed that the layer of snow deposited in a year on the surface compresses by 0.50 to 0.75 at 140 m depth at the drilling point. Reconstructed accumulation rates in the late Little Ice Age were slightly less than, or almost the same, as today. The highest reconstructed accumulation rates, at ~ 1810–1850, 1910 and 1970, coincide with glacier advances and mass balance changes in glaciers in Kamchatka (Solomina et al., 1995; Yamaguchi et al., 2008). One of the large uncertainties is the different firn/ice rheology employed in the two models. Glaciological observations of firn properties at the site and transient simulations using a firn layer model would improve the accumulation reconstruction.

The correlation map of δD with surface temperature data-sets and a comparison with the NPGO index implies that δD reflects NPGO data contained in the record. The significant negative correlation in the map between reconstructed accumulation rates and subpolar Northeast Pacific surface temperature as δD point to a strong relationship between precipitation conditions in this area and long-term climate change in the North Pacific.

The δD isotope and accumulation rate showed significant decadal and multi-decadal oscillation and changes of multi-decadal time periods in the mid to late 19th century. The time at which the multi-decadal oscillation signal in δD was lost coincided with changes in its average value between the end of the Little Ice Age and the present. The reconstructed accumulation records showed the shift of dominant periods around 1850 which is also present in paleo-climatic records from the Northeast Pacific. The similarity of the Ushkovsky/K2 ice core data and paleoclimate records from the Northeast Pacific coast indicate that the climatic changes of the mid-19th century in this region affected precipitation conditions in both the Northwest and Northeast Pacific.

Long-term isotope climate modelling will enhance further understanding of the relationship between δD data and the NPGO, NPGO reconstruction and the cause of its increase between the end of 19th to the early 20th century. Moreover, including both Northwest and Northeast Pacific paleoclimate data is necessary for a clearer understanding of the North Pacific climate and its changes between the Little Ice Age and the present.

Acknowledgements. We thank Yaroslav Murav'yev for his support of the ice core project, Sumito Matoba for guidance on water isotope measurements at the Institute of Low Temperature Science, Hokkaido University, and Jessica Lundin for helpful discussions and for checking the manuscript. ECMWF ERA-40 data used in this study were obtained from the ECMWF Data Server (http://data-portal.ecmwf.int/). The wavelet software was provided by Christopher Torrence and Gilbert P. Compo (http://atoc.colorado.edu/research/wavelets). Language editing of the manuscript was done by Andrew Davis of English Experience Language Services (Jena, Germany). Support by Grants-in-Aid for Scientific Research B (Nos. 16403005 and 19340137) from the Japan Society for the Promotion of Science JSPS is gratefully acknowledged. This publication is contribution no. 12 of the Nordic Centre of Excellence SVALI, "Stability and Variations of Arctic Land Ice", funded by the Nordic Top-Level Research Initiative (TRI).

References

Biondi, F., Gershunov, A., and Cayan, D. R.: North Pacific decadal climate variability since 1661, J. Climate, 14, 5–10, 2001. 2155

Bond, N. A., Overland, J. E., Spillane, M., and Stabeno, P.: Recent shifts in the state of the North Pacific, Geophys. Rev. Lett., 30, 2183, doi:10.1029/2003GL018597, 2003. 2163

Cecil, L. D., Green, J. R., and Thompson, L. G.: Earth Paleoenvironments: Records Preserved in Mid- and Low-latitude Glaciers, Springer, New York, 2004. 2154

Dansgaard, W.: Stable isotopes in precipitation, Tellus, 16, 436–468, 1964. 2164

D'Arrigo, R., Villalba, R., and Wiles, G.: Tree-ring estimates of Pacific decadal climate variability, Clim. Dynam., 18, 219–224, 2001. 2155

Di Lorenzo, E., Schneider, N., Cobb, K. M., Franks, P. J. S., Chhak, K., Miller, A. J., McWilliams, J. C., Bograd, S. J. Arango, H. Curchitser, E. Powell, T. M., and Rivière, P.: North Pacific Gyre Oscillation links ocean climate and ecosystem change, Geophys. Res. Lett., 35, L08607, doi:10.1029/2007GL032838, 2008. 2155, 2163

Di Lorenzo, E., Cobb, K., Furtado, J., Schneider, N., Anderson, B., Bracco, A., Alexander, M., and Vimont, D.: Central Pacific El Niño and decadal climate change in the North Pacific Ocean, Nat. Geosci., 3, 762–765, 2010. 2163

Durand, G., Gagliardini, O., Zwinger, T., Le Meur, E., and Hindmarsh, R. C. A.: Full Stokes modeling of marine ice sheets: influence of the grid size, Ann. Glaciol., 50, 109–114, 2009. 2159

Fisher, D. A., Wake, C., Kreutz, K., Yalcin, K., Steig, E., Mayewski, P., Anderson, L., Zheng, J., Rupper, S., Zdanowicz, C., Demuth, M., Waszkiewicz, M., Dahl-Jensen, D., Goto-Azuma, K., Bourgeois, J. B., Koerner, R. M., Sekerka, J., Osterberg, E., Abbott, M. B., Finney, B. P., and Burns S. J.: Stable isotope records from Mount Logan, Eclipse ice cores and nearby Jellybean Lake. Water cycle of the north Pacific over 2000 years and over five vertical kilometres: sudden shifts and tropical connections, Géogr. Phys. Quaternaire, 58, 337–352, doi:10.7202/013147ar, 2004. 2155, 2165

Furtado, J., Di Lorenzo, E., Schneider, N., and Bond, N.: North Pacific decadal variability and climate change in the IPCC AR4 models, J. Climate, 24, 3049–3067, 2011. 2163

Gagliardini, O. and Meyssonnier, J.: Flow simulation of a firn-covered cold glacier, Ann. Glaciol., 24, 242–248, 1997. 2159

Gagliardini, O. and Zwinger, T.: The ISMIP-HOM benchmark experiments performed using the Finite-Element code Elmer, The Cryosphere, 2, 67–76, doi:10.5194/tc-2-67-2008, 2008. 2159

Gedalof, Z. and Smith, D.: Interdecadal climate variability and regime-scale shifts in Pacific North America, Geophys. Res. Lett., 28, 1515–1518, 2001. 2165

Gray, S. T., Betancourt, J. L., Fastie, C. L., and Jackson, S. T.: Patterns and sources of multidecadal oscillations in drought-sensitive tree-ring records from the central and southern Rocky Mountains, Geophys. Res. Lett., 30, 1316, doi:10.1029/2002GL016154, 2003. 2165

Hagemann, R., Nief, G., and Roth, E.: Absolute isotopic scale for deuterium analysis of natural waters. Absolute D/H ratio for SMOW, Tellus, 22, 712–715, 1970. 2157

Hodge, S. M., Trabant, D. C., Krimmel, R. M., Heinrichs, T. A., March, R. S., and Josberger, E. G.: Climate variations and changes in mass of three glaciers in western North America, J. Climate, 11, 2161–2179, 1998. 2155

Holdsworth, G., Krouse, H. R., Nosal, M., Spencer, M. J., and Mayewski, P. A.: Analysis of a 290-year net accumulation time series from Mt. Logan, Yukon, in: Snow Cover and Glacier

Variations – Proceedings of the Baltimore Symposium, Maryland, May 1989, IAHS Publication No. 183, International Association of Hydrological Sciences, 71–79, 1989. 2155, 2165

Jacoby, G., Solomina, O., Frank, D., Eremenko, N., and D'Arrigo, R.: Kunashir (Kuriles) Oak 400-year reconstruction of temperature and relation to the Pacific Decadal Oscillation, Palaeogeogr. Palaeocl., 209, 303–311, 2004. 2155

Lipenkov, V. Y., Salamatin, A. N., and Duval, P.: Bubbly-ice densification in ice sheets: II. Applications, J. Glaciol., 43, 397–407, 1997. 2158

Mantua, N. J. and Hare, S. R.: The Pacific decadal oscillation, J. Oceanogr., 58, 35–44, 2002. 2155

Mantua, N. J., Hare, S. R., Zhang, Y., Wallace, J. M., and Francis, R. C.: A Pacific interdecadal climate oscillation with impacts on salmon production, B. Am. Meteorol. Soc., 78, 1069–1080, 1997. 2155

Matoba, S., Shiraiwa, T., Tsushima, A., Sasaki, H., and Muravyev, Y.: Records of sea-ice extent and air temperature at the Sea of Okhotsk from an ice core of Mount Ichinsky, Kamchatka, Ann. Glaciol., 52, 44–50, 2011. 2154

Matsuoka, K., Horikawa, S., Shiraiwa, T., Muravyev, Y. D., Salamatin, A. N., Ovsyannikov, A. A., Maeno, H., and Ohi, M.: Radio echo soundings at the summit ice cap of the Ushkovsky volcano, Kamchatka, in: Cryospheric Studies in Kamchatka II – Proceedings of the International Workshop on Cryospheric Studies in Kamchatka, January 1998, edited by: Naruse, R., Institute of Low Temperature Science, Hokkaido University, 20–24, 1999. 2156

Minobe, S.: A 50–70 year climatic oscillation over the North Pacific and North America, Geophys. Res. Lett., 24, 683–686, 1997. 2155

Moore, G. W. K., Holdsworth, G., and Alverson, K.: Climate change in the North Pacific region over the past three centuries, Nature, 420, 401–403, 2002. 2155

Murav'yev, Y. D., Ovsyannikov, A. A., and Shiraiwa, T.: Activity of the northern volcano group according to drilling data in the Ushkovsky crater glacier, Kamchatka, J. Volcanol. Seismol., 1, 42–52, doi:10.1134/S0742046307010034, 2007. 2156, 2157, 2174

Numaguti, A.: Origin and recycling processes of precipitating water over the Eurasian continent: Experiments using an atmospheric general circulation model, J. Geophys. Res., 104, 1957–1972, 1999. 2164

Paterson, W. S. B. and Waddington, E. D.: Past precipitation rates derived from ice core measurements: methods and data analysis, Rev. Geophys., 22, 123–130, 1984. 2158

Raymond, C., Weertman, B., Thompson, L., Mosley-Thompson, E., Peel, D., and Mulvaney, R.: Geometry, motion and mass balance of Dyer Plateau, Antarctica, J. Glaciol., 42, 510–518, 1996. 2158

Salamatin, A. N. and Duval, P.: Creep flow and pressure relaxation in bubbly medium, Int. J. Solids Struct., 34, 61–78, 1997. 2158

Salamatin, A. N., Lipenkov, V. Y., and Duval, P.: Bubbly-ice densification in ice sheets: I. Theory, J. Glaciol., 43, 387–396, 1997. 2158

Salamatin, A. N., Murav'yev, Y. D., Shiraiwa, T., and Matsuoka, K.: Modelling dynamics of glaciers in volcanic craters, J. Glaciol., 46, 177–187, 2000. 2156, 2158

Schwerzmann, A., Funk, M., Blatter, H., Lüthi, M., Schwikowski, M., and Palmer, A.: A method to reconstruct past accumulation rates in alpine firn regions: A study on Fiescherhorn, Swiss Alps, J. Geophys. Res., 111, F01014, doi:10.1029/2005JF000283, 2006. 2158

Seddik, H., Greve, R., Zwinger, T., and Placidi, L.: A full Stokes ice flow model for the vicinity of Dome Fuji, Antarctica, with induced anisotropy and fabric evolution, The Cryosphere, 5, 495–508, doi:10.5194/tc-5-495-2011, 2011. 2159

Seddik, H., Greve, R., Zwinger, T., Gillet-Chaulet, F., and Gagliardini, O.: Simulations of the Greenland ice sheet 100 years into the future with the full Stokes model Elmer/Ice, J. Glaciol., 58, 427–440, doi:10.3189/2012JoG11J177, 2012. 2159

Shiraiwa, T. and Yamaguchi, S.: Reconstruction of glacier mass balances and climate changes in the Kamchatka Peninsula, J. Geogr. Tokyo, 111, 476–485, 2002. 2155, 2156, 2157, 2160, 2163

Shiraiwa, T., Muravyev, Y. D., and Yamaguchi, S.: Stratigraphic features of firn as proxy climate signals at the summit ice cap of Ushkovsky Volcano, Kamchatka, Russia, Arctic Alpine Res., 29, 414–421, 1997. 2156

Shiraiwa, T., Murav'yev, Y. D., Kameda, T., Nishio, F., Toyama, Y., Takahashi, A., Ovsyannikov, A. A., Salamatin, A. N., and Yamagata, K.: Characteristics of a crater glacier at Ushkovsky volcano, Kamchatka, Russia, as revealed by the physical properties of ice cores and borehole thermometry, J. Glaciol., 47, 423–432, 2001. 2154, 2155, 2156

Shiraiwa, T., Goto-Azuma, K., Matoba, S., Yamasaki, T., Segawa, T., Kanamori, S., Matsuoka, K., and Fujii, Y.: Ice core drilling at King Col, Mount Logan 2002, B. Glaciol. Res., 20, 57–63, 2003. 2155

Solomina, O. N., Muravyev, Y. D., and Bazanova, L. I.: "Little Ice Age" glaciers in Kamchatka, northeastern Russia, Ann. Glaciol., 21, 240–244, 1995. 2163, 2166

Steig, E. J., Grootes, P. M., and Stuiver, M.: Seasonal precipitation timing and ice core records, Science, 266, 1885–1886, doi:10.1126/science.266.5192.1885, 1994. 2162

Torrence, C. and Compo, G. P.: A practical guide to wavelet analysis, B. Am. Meteorol. Soc., 79, 61–78, 1998. 2164, 2180, 2181

Wagenbach, D.: Environmental records in Alpine glaciers, in: The Environmental Record in Glaciers and Ice Sheets, edited by: Oeschger, H. and Langway, C. C., John Wiley & Sons, Chichester, 69–83, 1989. 2154

Wake, C. P., Yalcin, K., and Gundestrup, N. S.: The climate signal recorded in the oxygen-isotope, accumulation and major-ion time series from the Eclipse ice core, Yukon Territory, Canada, Ann. Glaciol., 35, 416–422, 2002. 2155

Yamaguchi, S., Naruse, R., and Shiraiwa, T.: Climate reconstruction since the Little Ice Age by modelling Koryto glacier, Kamchatka Peninsula, Russia, J. Glaciol., 54, 125–130, 2008. 2163, 2166

Yasunari, T. J., Shiraiwa, T., Kanamori, S., Fujii, Y., Igarashi, M., Yamazaki, K., Benson, C. S., and Hondoh, T.: Intra-annual variations in atmospheric dust and tritium in the North Pacific region detected from an ice core from Mount Wrangell, Alaska, J. Geophys. Res., 112, D10208, doi:10.1029/2006JD008121, 2007. 2155

Zwinger, T. and Moore, J. C.: Diagnostic and prognostic simulations with a full Stokes model accounting for superimposed ice of Midtre Lovénbreen, Svalbard, The Cryosphere, 3, 217–229, doi:10.5194/tc-3-217-2009, 2009. 2159

Zwinger, T., Greve, R., Gagliardini, O., Shiraiwa, T., and Lyly, M.: A full Stokes-flow thermo-mechanical model for firn and ice applied to the Gorshkov crater glacier, Kamchatka, Ann. Glaciol., 45, 29–37, doi:10.3189/172756407782282543, 2007. 2156, 2159, 2160, 2161

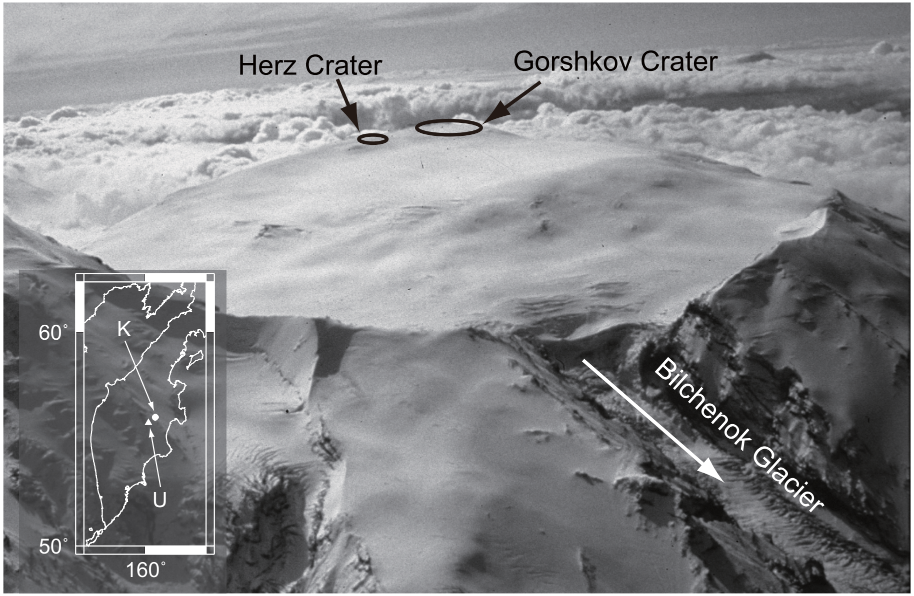

Fig. 1. The north face of Ushkovsky volcano and the summit craters. Bilchenok Glacier is the main outlet from the summit ice cap. Inset the location of Ushkovsky volcano (U) and the nearby weather station, Kljuchi (K).

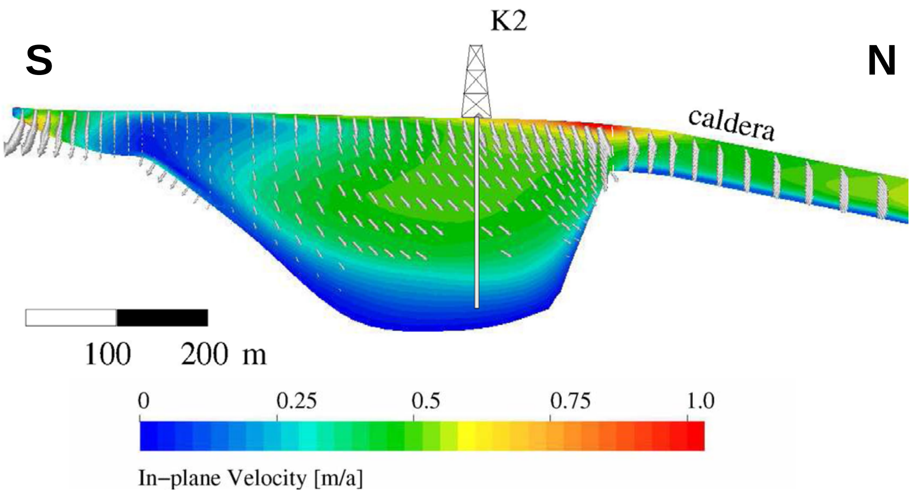

Fig. 2. Velocity field (absolute values as texture and direction vectors) simulated with Elmer/Ice in a north-south transect of the Gorshkov crater glacier through the K2 drillsite.

CPD
9, 2153–2181, 2013

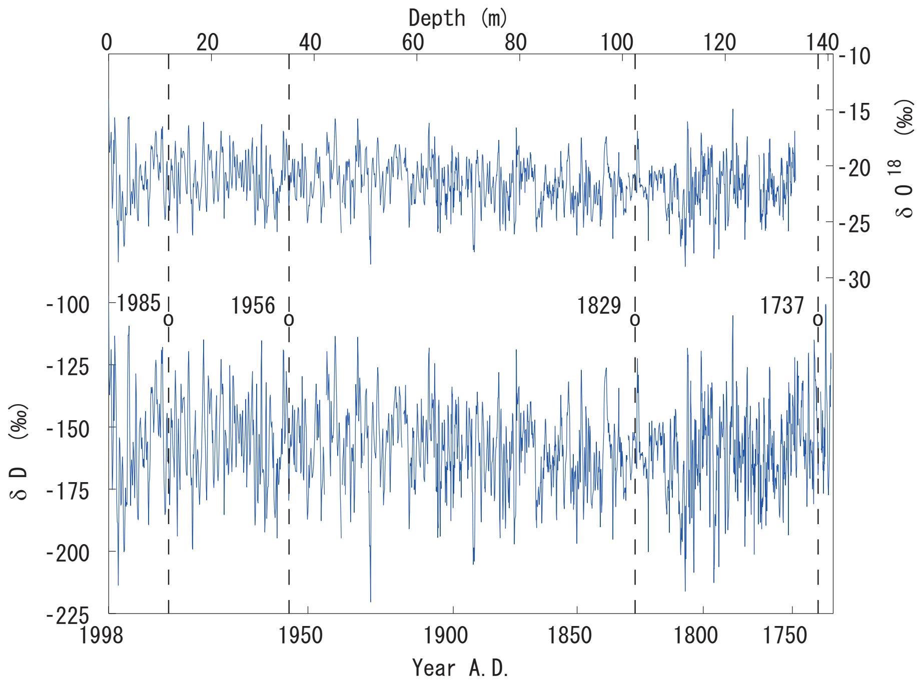

Fig. 3. Measured water isotope profiles with dating results. Upper line: $\delta^{18}O$, lower line: δD. Dotted lines with year number indicate dated volcanic ash layers (Murav'yev et al., 2007).

CPD
9, 2153–2181, 2013

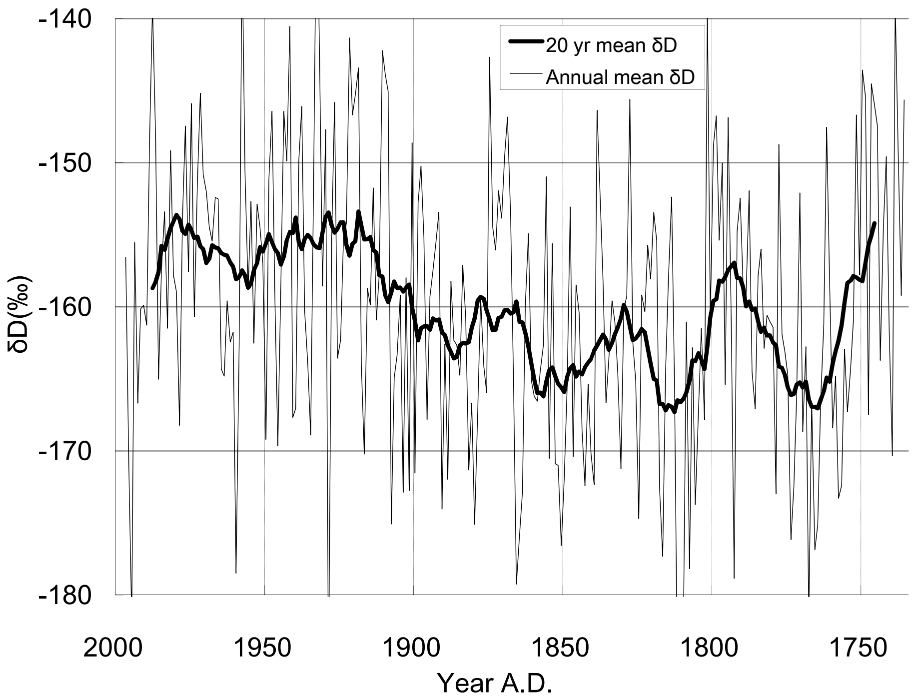

Fig. 4. Annual mean (thin line) and 20 yr mean (thick line) δD profiles. Note that the average isotope ratio increases from the late 19th to the early 20th century.

CPD
9, 2153–2181, 2013

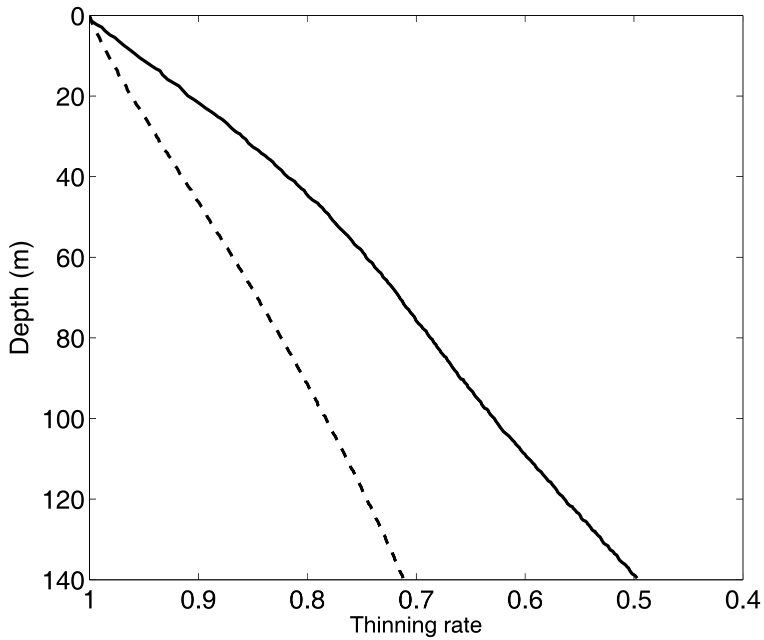

Fig. 5. Thinning rates calculated by the Salamatin (dotted line) and Elmer/Ice (solid line) models.

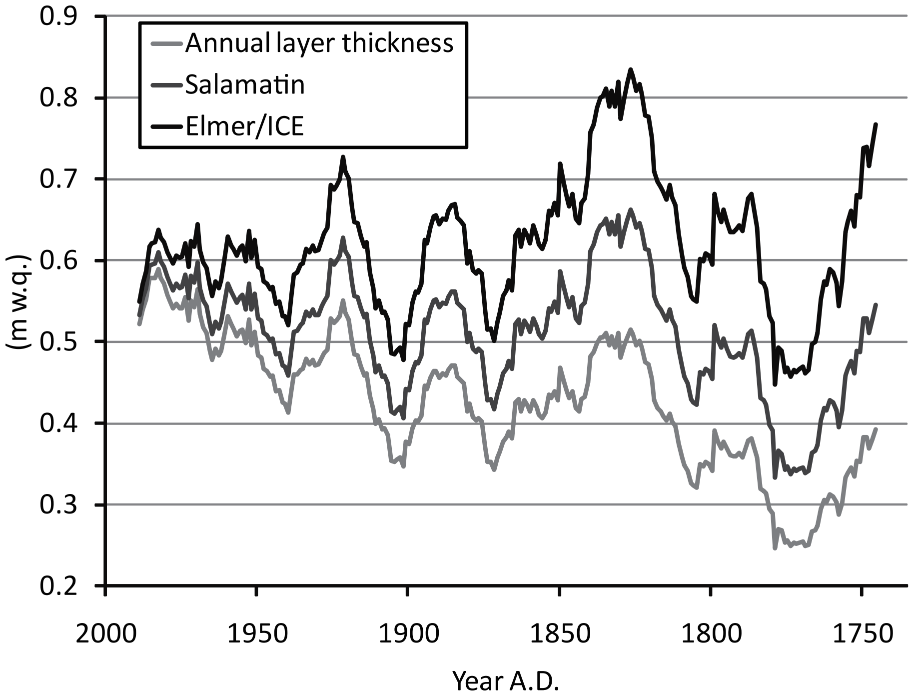

Fig. 6. Reconstructed 20 yr mean accumulation rates and annual layer thickness profiles.

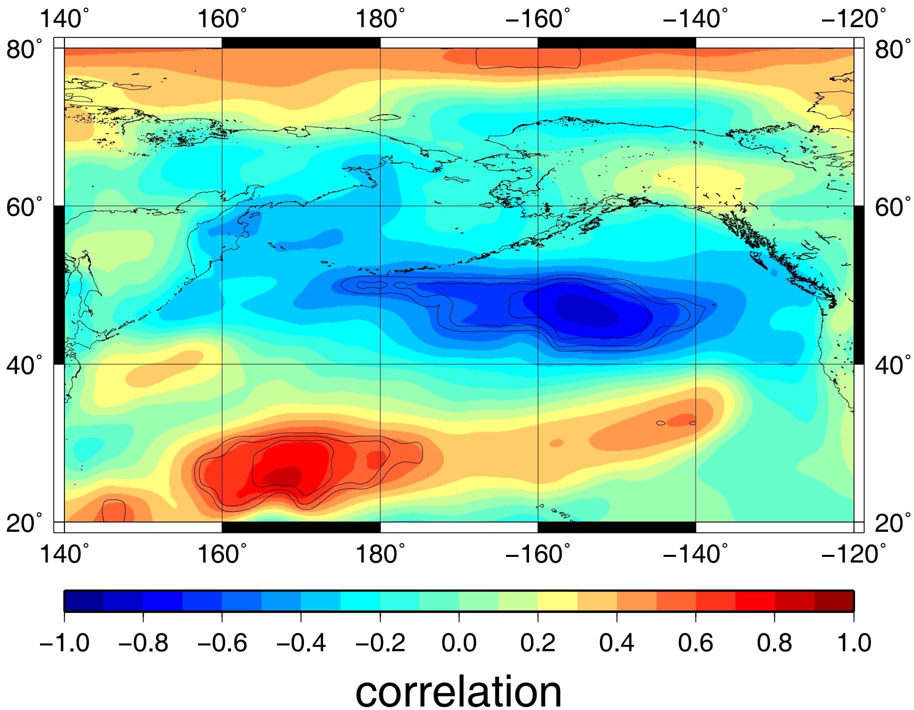

Fig. 7a. Correlation map of the ice core δD with ERA40 3 yr mean surface (2 m) temperature. Black contours indicate the land-water margin and the 90, 95 and 99 % confidence levels.

CPD
9, 2153–2181, 2013

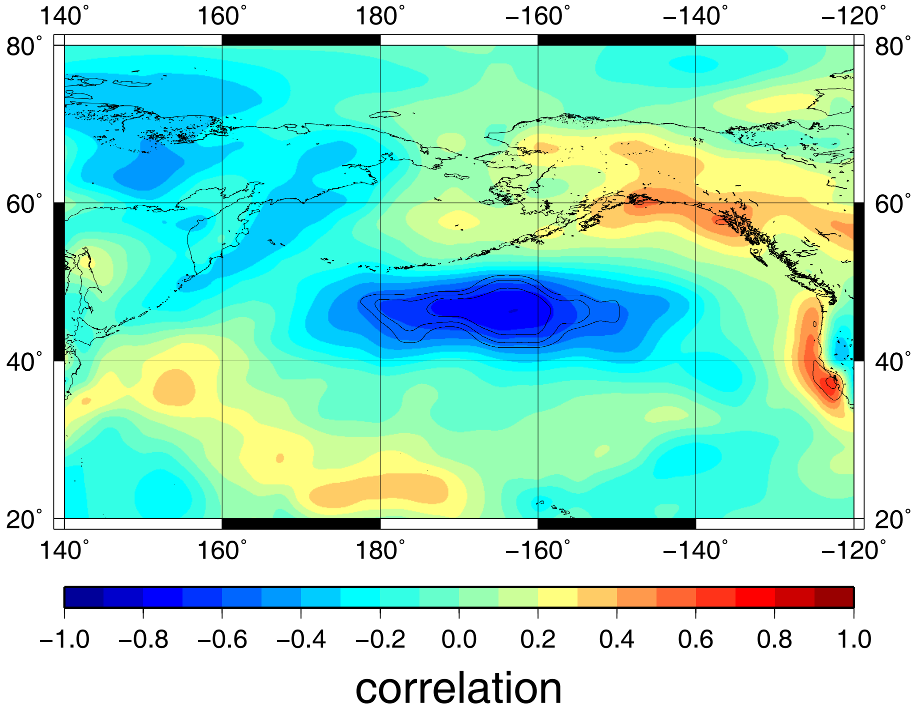

Fig. 7b. Correlation map of reconstructed accumulation rates (Elmer/Ice) with ERA40 3 yr mean surface (2 m) temperature. Black contours indicate the land-water margin and the 90, 95 and 99 % confidence levels.

CPD
9, 2153–2181, 2013

Ice core from the Ushkovsky volcano, Kamchatka

T. Sato et al.

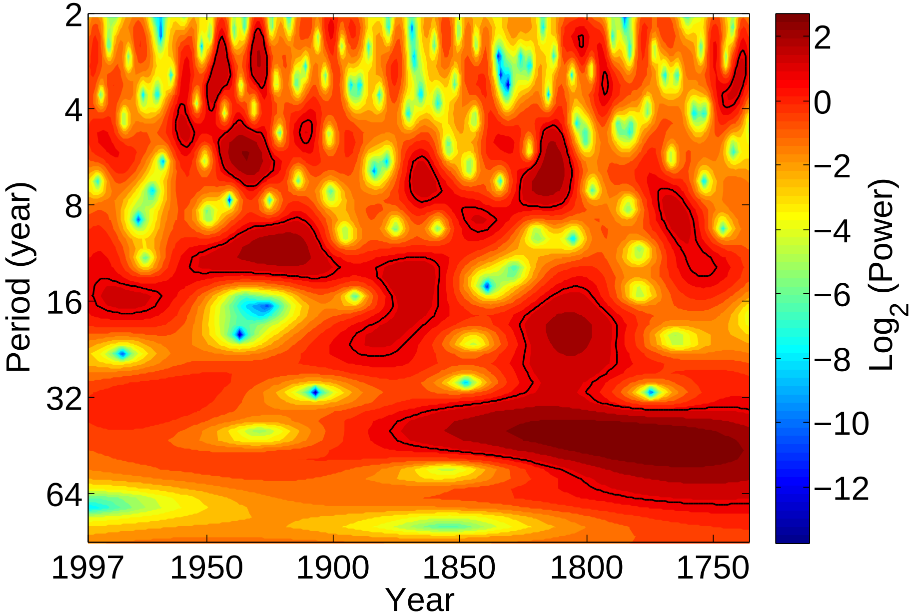

Fig. 8a. Wavelet plot for δD: binary logarithm of the power (absolute square of the wavelet transform) in ‰^{2}. Black contours represent the 95 % confidence level against red noise (Torrence and Compo, 1998).

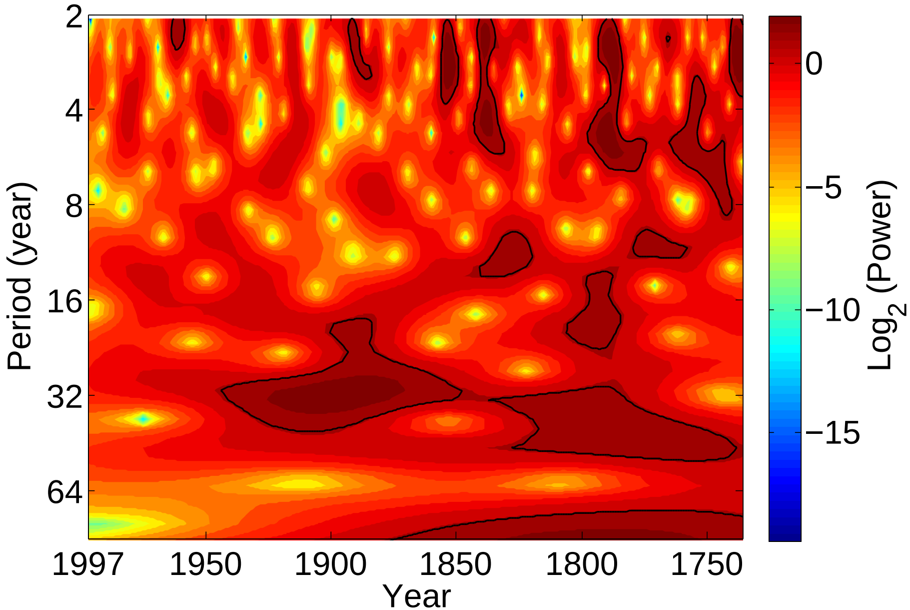

Fig. 8b. Wavelet plot for reconstructed accumulation rates (Elmer/Ice): binary logarithm of the power (absolute square of the wavelet transform) in $m^2 a^{-2}$. Black contours represent the 95 % confidence level against red noise (Torrence and Compo, 1998).